JOURNAL OF THERMOPHYSICS AND HEAT TRANSFER
Vol. 7, No. 2, April–June 1993

Experimental Investigation of an Ion-Drag Pump-Assisted Capillary Loop

B. R. Babin,* G. P. Peterson,† and J. Seyed-Yagoobi‡
Texas A&M University, College Station, Texas 77843

An ion-drag pump was constructed and calibrated to determine the available pumping pressure as a function of input voltage for various working fluids. The experimental results were then compared with an analytical model and found to predict the ion-drag pump performance to within ±15%. Using this information, an analytical model capable of predicting the performance enhancement of an ion-drag pump-assisted capillary loop was also developed and compared with the values obtained from experimental tests conducted on a thermal test loop. Although the analytical model slightly overpredicted the performance enhancement resulting from the ion-drag pump, the predicted trends were similar to those obtained from the experimental program. These trends included decreased thermal test loop performance with increased evaporator/condenser elevation difference, increased performance (due to increased operating temperature), and an increase in performance ranging from 20 to 100%, due to the addition of a two-stage ion-drag pump. The performance enhancement of the thermal test loop was verified at various operating temperatures and evaporator/condenser elevation differences.

Nomenclature

d	=	diameter
g	=	gravitational acceleration
h	=	evaporator/condenser height difference
I	=	current
L	=	length
Me	=	merit number
P	=	pressure
Q	=	heat transport capacity
r	=	radius
V	=	voltage
δ	=	emitter/collector electrode spacing
ε	=	dielectric constant
η	=	efficiency
Θ	=	wetting angle
λ	=	latent heat
μ	=	viscosity
$\dot{v}$	=	volumetric flow rate
ρ	=	density
σ	=	surface tension
ϕ	=	angle of inclination

Subscripts

c	=	capillary
EHD	=	electrohydrodynamic
g	=	gravitational
l	=	liquid
v	=	vapor
0	=	charge

Introduction

THE capillary limit in a heat pipe or two-phase capillary pumped loop, occurs when the capillary pumping pressure is not sufficient to promote flow of the working fluid from the condenser back to the evaporator. This problem occurs in the large monogroove heat pipes proposed for use on the Space Station Freedom[1] and also in the tiny micro heat pipes used for the thermal control of semiconductor devices.[2] Because the capillary pumping capacity is the primary limitation which governs the operation of most moderate temperature heat pipes and capillary loops, numerous alternative pumping mechanisms have been proposed and evaluated for use in these devices. These alternative pumping mechanisms include the development of complex arterial wicking structures such as the monogroove,[1] the double wall artery,[3] or the cats eye artery[4]; and the investigation of various active pumping mechanisms such as osmotic, bimorph, and mechanical pumps[5,6]; or the use of a vapor compressor.[7] These various capillary enhancement and active pumping mechanisms have been evaluated and compared previously,[7] and while the arterial modifications have proven quite successful, several of the active pumping mechanisms have experienced problems associated with vibrations and/or size limitations. One relatively new pumping mechanism under investigation for these types of applications is the electrohydrodynamic (EHD) pump. Electrohydrodynamic pumping results from the application of an electrical field to a dielectric fluid. As shown in Fig. 1, free charges are established within the dielectric fluid by emission of a corona source. The electrical field created by the negatively energized emitter electrode and the grounded collector electrode drags the free charges through the field, thus setting the fluid in motion. These types of electrohydrodynamic pumps are known as ion-drag pumps.

The fundamental physical phenomena which makes the operation of ion-drag pumps possible was first described in the early 1900s.[8] Later in the 1950s, a significant number of experimental and analytical advances were made. The analytical modeling was particularly useful because it facilitated further

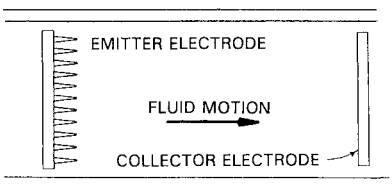

Fig. 1 Ion-drag pump operating mechanism.

Presented as Paper 91-1401 at the AIAA 25th Thermophysics Conference, Honolulu, HI, June 24–26, 1991; received June 28, 1991; revision received June 6, 1992; accepted for publication June 9, 1992.

*Graduate Research Assistant, Department of Mechanical Engineering.

†Tenneco Professor of Engineering, Department of Mechanical Engineering. Associate Fellow AIAA.

‡Associate Professor of Mechanical Engineering, Department of Mechanical Engineering.

pump development and research.[9] These analytical and experimental developments continue to be the foundation of a majority of the work done in this field.

In the early 1970s Abu-Romia[10] suggested the use of electro-osmotic forces to assist in the pumping of liquid in a capillary driven heat pipe. In an extension of this concept, Jones[11] proposed a new type of heat pipe which utilized an electrode structure to orient and guide the dielectric liquid flow. The results of this investigation indicated that relatively high performance devices were possible.

Ion-drag pumps have no moving parts and as a result will not create any of the vibration problems typically associated with conventional rotary pumps or compressors. They have been shown to be capable of providing continuous pumping pressures for several traditional heat pipe working fluids (i.e., dielectric refrigerants),[12-14] require low power input, have a pump power efficiency ($\eta = \dot{v}\Delta P/VI$) of approximately 5–10%,[14] and appear to be well-suited as an alternative active pumping mechanism for use in heat pipe or capillary pumped systems. The objective of the present work was to determine the feasibility and possible performance enhancement which could result from the use of an ion-drag pump designed to supplement the capillary pumping of the wicking structure within operating heat pipes or capillary pumped loops. In this way, the capillary limit could be increased and the axial heat transport improved.

Analytical Evaluation

Prior to the construction of the experimental test facility, it was first necessary to develop an analytical model capable of predicting the performance limitations and operational characteristics of a thermal test loop both with and without the assistance of an ion-drag pump. Once developed, this model could be used to select the working fluid and design the experimental test facility.

Modeling of Heat Pipe with Ion-Drag Pump Enhancement

To function properly, the capillary pumping pressure in a heat pipe or capillary pumped loop must be greater than or equal to the sum of the pressure losses throughout the loop. This can be stated mathematically as

$$\Delta P_c \geq \Delta P_v + \Delta P_l + \Delta P_g \tag{1}$$

where ΔP_c is the capillary pumping pressure, ΔP_v is the pressure required to transport the vapor from the evaporator to the condenser, ΔP_l is the pressure required to transport the liquid from the condenser to the evaporator, and ΔP_g is the hydrostatic pressure due to the local gravitational acceleration. Each of these pressure gradients can be expressed as functions of the physical structure of the heat pipe or capillary loop and the properties of the working fluid.

The first of these, the capillary pumping pressure, can be defined mathematically as

$$\Delta P_c = (2\sigma/r_c)\cos\theta \tag{2}$$

where r_c is the capillary radius of the wicking structure. The pressure gradient occurring in the vapor and liquid passages can be expressed as

$$\Delta P_v = (2f/d_v^2\rho_v^2\lambda^2)L_vQ^2 \tag{3}$$

$$\Delta P_l = (128\mu_l/\pi d_l^4\rho_l\lambda)L_lQ \tag{4}$$

respectively, as presented by Chi.[15] Finally, the hydrostatic pressure term ΔP_g can be expressed as

$$\Delta P_g = \rho_l g L_l \sin\phi \tag{5}$$

where ϕ is the angle of the liquid return passage with respect to a plane normal to the gravitational vector. This term may either assist or hinder the return of the liquid from the condenser to the evaporator, or in space applications where the gravitational acceleration is near zero may be negligible.[16]

When an ion-drag pump is utilized to assist in the return of liquid from the condenser to the evaporator, an additional term must be added to Eq. (1) to account for the increased pumping pressure. The resulting expression for the capillary limit of an ion-drag assisted heat pipe or capillary pumped loop then becomes

$$\Delta P_c + \Delta P_{\text{EHD}} \geq \Delta P_v + \Delta P_l + \Delta P_g \tag{6}$$

where ΔP_{EHD} represents the available pumping pressure provided by the ion-drag pump. This available pumping pressure can be approximated in terms of the applied voltage and the maximum uniform charge density as

$$\Delta P_{\text{EHD}} = \rho_0 V \tag{7}$$

The maximum charge density within the generated electrical field in these types of devices has been shown to be[17]

$$\rho_0 \leq (2\varepsilon V/\delta^2) \tag{8}$$

Utilizing the expression given in Eq. (6), the maximum Q for an ion-drag pump assisted heat pipe or capillary pumped loop can be developed as a function of the physical structure of the loop, the properties of the working fluid, and the electrical field applied to the ion-drag pump.

Selection of Working Fluid

With the merging of two separate phenomena (heat pipes/capillary pumped loops and ion-drag pumps) as was done in this investigation, careful consideration must be given to the working fluid. The working fluid must be useful as a heat pipe fluid, i.e., have a large latent heat of vaporization, low viscosity, and high surface tension, and also must have a low electrical conductivity and a high permeativity.[18] To determine the performance of different heat pipe working fluids, *Me* defined as

$$Me = (\rho_l\sigma_l\lambda/\mu_l) \tag{9}$$

can be used.[16]

After considering several potential working fluids, R11 was selected due to the combination of low electrical conductivity and relatively high merit number.

Experimental Apparatus

To conduct the experimental investigation, three major components were constructed: 1) an ion-drag pump, 2) a pump calibration facility, and 3) a thermal test loop. Each of these components is discussed separately in the following sections.

Ion-Drag Pump

A schematic of the ion-drag pump used in the current investigation is shown in Fig. 2. The pump was constructed from a Lexan® tube with an outer diameter of 2.54 cm and inner diameter of 1.90 cm. Two sections, each 2-cm long, were cut for use in the construction of the emitter electrodes. A circumferential groove approximately 1-mm deep and 2-mm wide was then machined into the outer surface of each section, midway between the two ends.

A series of 0.61-mm diam holes were then drilled radially in the center of the groove at 10-deg increments producing a total of 36 holes per section. Brass needles 0.61-mm in diameter were inserted into each hole so that the tip of each needle penetrated approximately 2-mm past the interior wall of the Lexan tube. The needles were then sealed in place by injecting a dichloro-methane solution into the groove. Next, the needles were bent in the flow direction using a specially designed fixture, and copper wire was woven through the

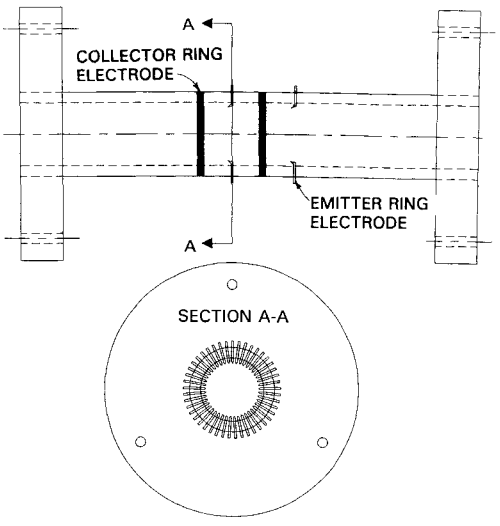

Fig. 2 Construction of an ion-drag pump.

protruding outer ends of the needles until the grooves were filled. In this manner, an electrical connection between all of the needles was achieved.

Two collector electrodes, also shown in Fig. 2, were fabricated from a 2.54-cm diam brass rod with a 1.90-cm hole machined in the center. The resulting brass tube was cut into slices 2-mm long, and as was the case for the collector electrodes, a small groove was machined into the outer surface and copper wire was wrapped around the emitter electrode to make the electrical connection. Once completed, the emitter and collector electrodes were assembled in an alternating pattern and glued together resulting in a two-stage pump with a distance of approximately 10.2 mm between the emitter and collector electrodes in each stage. A layer of corona dope was applied to all the exposed metallic parts to ensure that no electrical breakdown would occur on the external surfaces of the pump. Lexan connector flanges were then bonded to each end of the ion-drag pump so it could be attached to the pump calibration and thermal test loop facilities.

The electrodes in this ion-drag pump were designed with primary consideration given to the fluid mechanics occurring within the pump. For this reason, the emitter electrodes supplied the necessary charges within the viscous layers where the electrical forces were most useful in overcoming the high viscous shear stresses.

Pump Calibration Facility

In order to calibrate the ion-drag pump, a pump test facility was constructed. This facility consisted of a 9-cm diam U-tube connected by a smaller diameter test section bonded to each leg of the U-tube. The ion-drag pump was bolted between two flanges attached to this smaller tube and sealed with O-rings. Pressure taps were located 2.54 cm from each end of the ion-drag pump to measure the pressure difference generated by the pump to within ± 2.5 Pa as a function of the applied voltage, which was measured with an accuracy of ± 0.2 kV using a digital multimeter. In addition to measuring the pressure differential and voltage, a series of T-type thermocouples (AWG30) with an experimental uncertainty of ± 0.5°C were located in the liquid to monitor the temperature throughout the tests. Using this pump calibration facility, the pumping pressure of the ion-drag pump could be determined as a function of the input voltage applied to the emitter electrodes.

Thermal Test Loop

To test the performance enhancement of the ion-drag pump, the thermal test loop shown in Fig. 3 was constructed. This thermal test loop consisted of three primary components: 1) an evaporator, 2) a condenser, and 3) the vapor/liquid channels. The evaporator and condenser were both made from 20.32 × 20.32 × 3.17 cm copper blocks. The centers of the blocks were machined to form 17.78 × 17.78 × 2.54 cm open sections as shown in Figs. 4a and 4b. The evaporator had a 1-mm deep groove, 3-mm high, cut along the bottom surface to hold down three layers of no. 12 mesh copper screen. Approximately 1 m of 0.635-cm coiled copper tubing was installed in the condenser through which an ethylene-glycol coolant was circulated. To seal both the evaporator and the condenser, a 20.32 × 20.32 × 0.635 cm copper lid was silver soldered to each of the base plates. Holes were drilled

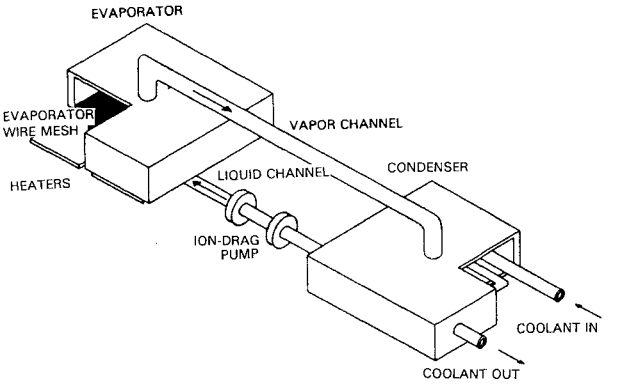

Fig. 3 Schematic of the thermal test loop facility.

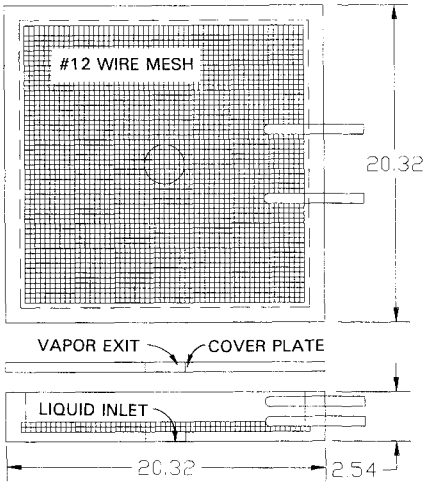

a) Evaporator construction

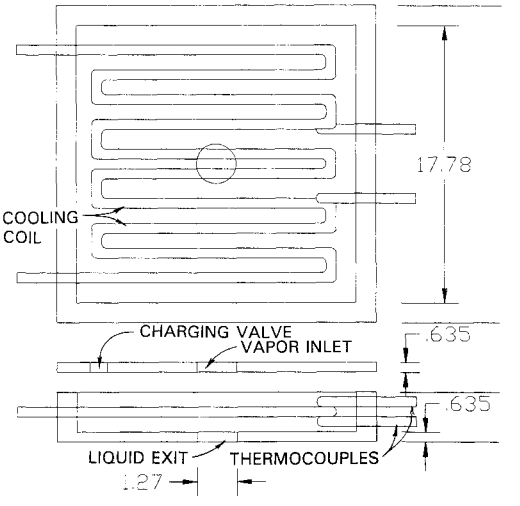

b) Condenser construction

Fig. 4 Centers of copper blocks machined to form 17.78 × 2.54 cm open sections.

and tapped in the lid of the condenser for a valve to be used to charge the heat pipe.

The liquid and vapor flow channels were installed in 1.27-cm diam holes drilled into the top and bottom of both the condenser and evaporator. The vapor and liquid flow channels, 1.27-mm diam. and 2.5-m long, were then silver soldered in the top and bottom of the evaporator and condenser. The lower channel, which served as the liquid return line, was fitted with two Lexan connector flanges to allow the installation of the ion-drag pump. The entire test loop including the condenser, evaporator, and flow channels was then wrapped with Fiberglas® insulation approximately 10-cm thick to reduce the convective losses.

To insure proper wetting, the thermal test loop was cleaned using an acetone solution. After cleaning, the test loop was evacuated and rinsed several times with *n*-Propyl alcohol. The test loop was again evacuated and charged with 1.6 l of R11. The charging procedure was accomplished in such a manner so as to minimize the amount of noncondensible gases admitted to the system.

Experimental Procedure

In order to investigate the effects of the ion-drag pump on the thermal test loop, a series of three separate tests were conducted. First, the ion-drag pump was calibrated in order to develop a pump calibration curve which described the relationship between the input voltage and pump pressure for the R11 working fluid. Second, the thermal test loop was evaluated without the ion-drag pump to determine the maximum transport capacity. And third, the ion-drag pump was placed in the thermal test loop to determine the increase in the heat transport capacity resulting from the ion-drag pump.

During the ion-drag pump pressure calibration tests, the input voltage to the emitter electrodes was varied, and the input voltage and current were measured using two digital multimeters. The resulting pressure difference generated by the ion-drag pump was measured by two pressure taps located at the pump inlet and exit and a differential pressure transducer. As mentioned previously, because the pumping pressure is a function of the working fluid properties, and therefore, temperature dependent, several thermocouples were placed in the working fluid to monitor the temperature throughout the pump calibration tests.

The pump calibration tests were conducted as follows: the test facility was filled with refrigerant R11 and the system was sealed. A data acquisition system control program was then initiated and measurements of the temperature and the pressure differential produced by the ion-drag pump were recorded for 3 min at 15-s intervals. The mean pressure differential and standard deviation were then calculated and stored. This process was repeated, increasing the voltage to the ion-drag pump from 10 to 26 kV in increments of 2 kV. This provided a method by which the pumping pressure generated by the ion-drag pump could be determined to within ± 2.5 Pa.

Once the ion-drag pump pressure differential had been established as a function of the input voltage, the ion-drag pump was installed in the thermal test loop as illustrated in Fig. 3. In this test loop, input power was provided to the evaporator by two 7.6 × 17.8 cm electrical resistance heaters and measured by monitoring the voltage and current. Heat removal from the condenser was provided by a constant temperature circulating bath, and measured using two thermocouples placed at the coolant flow inlet and outlet to calculate the sensible heat of the ethylene-glycol coolant. To monitor the temperatures in the heat pipe, several T-type sheathed thermocouples were installed in the vapor and liquid space of both the evaporator and condenser. Three other thermocouples (T-type, AWG-30) were embedded in the bottom of the casing of both the evaporator and condenser at 1.27-cm intervals from the center. Throughout the thermal tests, the input power to the ion-drag pump and pressure differential were again measured using the technique previously described for the pump calibration tests.

The thermal test loop investigation was conducted as follows: The coolant bath temperature was adjusted and once the system had reached a constant temperature, the control program was initiated. This program continuously displayed the previously mentioned measured quantities at 15-s intervals. The heat pipe was then situated in a horizontal position and an input heat flux was applied to the evaporator. After the system had reached steady state, the evaporator was slightly elevated. This process was then repeated until evaporator dryout (defined as the point where the condenser vapor temperature steadily decreased while the evaporator vapor temperature continued to rise) had been reached. At this point the ion-drag pump was turned on and the effect on the thermal transport capacity was observed. The elevation was again incremented until the point at which dryout occurred. Once a set of tests had been completed, the system was allowed to cool and the process was repeated for increasing power intervals and then again for varying condenser coolant temperatures.

Results and Discussion

Using Eq. (7), the pressure generated by the ion-drag pump was determined for the two-stage pump. Additional estimations for three and four stage ion-drag pumps of similar construction have been presented by Babin.[19] For all three cases the pressure generated by the ion-drag pump increased linearly with increasing voltage. Figure 5 illustrates the results obtained for a two-stage pump. The experimental data resulting from the ion-drag pump pressure tests are also illustrated in Fig. 5. As shown, the model predicts the performance of the ion-drag pump reasonably well. However, the slope of the predicted curve is approximately 10% less than the slope of the experimental curve. Overall, the analytical model of the pump performance proved to be a good indicator of the actual pump performance.

Using the heat pipe modeling technique previously described, the thermal test loop performance, both with and without the ion-drag pump, was determined as a function of the evaporator/condenser elevation difference for various operating temperatures. The results indicate that the thermal transport capacity of the test loop increases with increased operating temperature, and that the effect of elevation difference is slightly greater at higher temperatures. Figure 6 illustrates the improvement in the transport capacity predicted by the analytical model presented in Eq. (6), using a two-stage ion-drag pump with 12 kV (20 Pa, see Fig. 5) and an operating temperature of 265 K. As illustrated, the model predicts a 40% performance increase at zero elevation difference. Also, the elevation at which the thermal test loop ceases to operate increased from 3 to 4.75 mm, a 50% improvement over that of the thermal test loop without ion-drag pump.

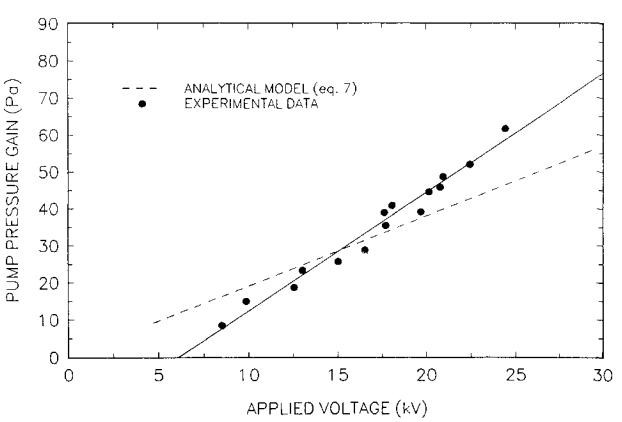

Fig. 5 Comparison of analytical and experimental performance for a two-stage ion-drag pump at 265 K.

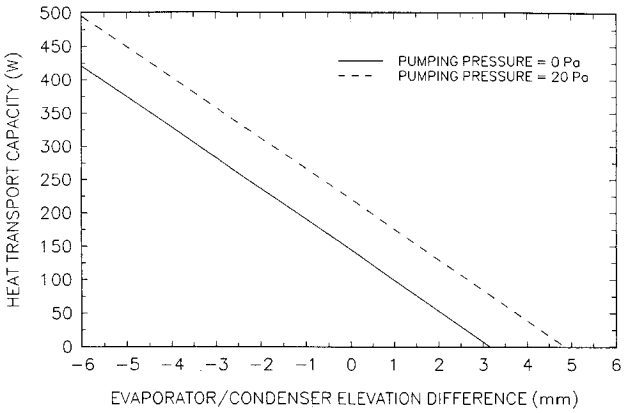

Fig. 6 Predicted performance with and without two stage ion-drag pump enhancement at 265 K, 20 kV.

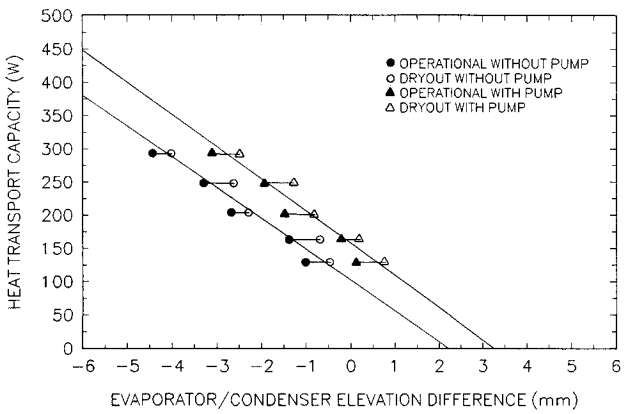

Fig. 7 Measured heat pipe performance with and without the two-stage ion-drag pump at 265 K, 20 kV.

The results of the experimental investigation of the ion-drag pump-assisted thermal test loop are shown in Fig. 7, for an operating temperature of 265 K. In this figure, the solid symbols indicate the last test point prior to dryout, while the open symbols represent the first point where dryout was confirmed. The arithmetic average of these two points was assumed to be the point where dryout occurred. The two solid lines represent a best-fit straight line through these dryout values. As shown, the performance enhancement due to the ion-drag pump was varied from almost 100% at high adverse tilts (evaporator up) to less than 20% when the thermal test loop was operating in a reflux mode. In addition, the maximum tilt at which the pump assisted thermal test loop would continue to operate was increased from approximately 2–3.5 mm. Finally, it is clear that the performance of the thermal test loop decreased as the tilt increased, verifying the effect of tilt on the test loop performance.

By comparing Figs. 6 and 7, it is apparent that the analytical heat transport model given by Eq. (6), overpredicted the performance of the thermal test loop both with and without the ion-drag pump by nearly the same amount. This would indicate that although not predicting the operational limit with a high degree of accuracy, the analytical model can be used as an effective tool in the design and optimization of these types of systems.

Another perspective of the thermal test loop performance enhancement due to ion-drag pumping can be gained by evaluating the data at a constant evaporator/condenser elevation difference (i.e., ϕ equals a constant) and varying the operating temperature. This is done in Fig. 8 which compares the predicted and measured performance of the thermal test loop both with and without the ion-drag pump. As illustrated, the model and experimental results demonstrate a similar improvement due to the addition of the ion-drag pump. Again, the model overpredicts the performance by approximately

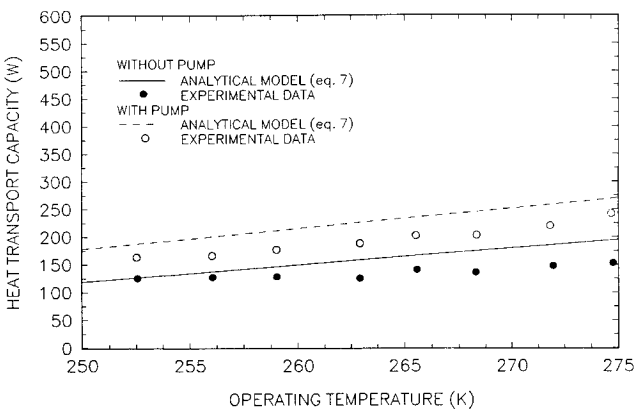

Fig. 8 Comparison of predicted and measured heat pipe performance in a horizontal orientation with and without the two-stage ion-drag pump, 20 kV.

20%, however, several conclusions can still be made. The first of these is that while the analytical model overpredicts the enhancement due to the ion-drag pump, the slopes of the curves are similar, again illustrating the practicality of the model in the design of such thermal test loops. The second conclusion is that for each operating temperature, a clearly visible enhancement in the performance occurred due to the ion-drag pump.

Finally, the input power to the ion-drag pump, which is on the order of 1.0 W for all of the tests reported here, was monitored throughout the experimental program by measuring the voltage and current levels. The measured power levels were consistent with other values previously reported for similar ion-drag pumps.[14]

Conclusions

An ion-drag pump that enhanced the performance of a thermal test loop was successfully constructed and operated. This ion-drag pump was experimentally calibrated to determine the pumping pressure generated as a function of input voltage. The results were then compared to an analytical model, which was shown to predict the ion-drag pumping pressure as a function of input voltage and fluid properties to within $\pm 15\%$. Additional work on the construction of ion-drag pumps is necessary if they are to be developed to operate in more complex heat transfer systems, such as heat pipes or capillary pumped loops.

An analytical model that predicts the performance enhancement of a thermal test loop due to the addition of an ion-drag pump has also been developed. Experimental results compared favorably with the values predicted by this model. Although the analytical model slightly overpredicted the performance enhancement of the thermal test loop, it illustrates trends similar to those of the experimental data. These trends include decreased performance with increasing evaporator/condenser elevation difference, increased performance due to increasing operating temperature, and a significant increase in the performance due to the inclusion of the ion-drag pump. Most significantly, an ion-drag pump suitable for use in heat pipes or capillary pumped loops have been constructed and tested, and shown to improve the heat transport capacity from 20 to 100% with two electrode pairs. This performance enhancement was verified at various operating temperatures and evaporator/condenser elevation differences. Greater improvement in the heat transport capacity and pressure generation can be achieved by increasing the number of the energized electrode pairs with only a small increase in the required input power.[14]

References

[1]Alario, J., Haslett, R., and Kosson, R., "The Monogroove High Performance Heat Pipe," AIAA Paper 81-1156, June 1981.

[2]Babin, B. R., Peterson, G. P., and Wu, D., "Steady-State Modeling and Testing of a Micro Heat Pipe," *Journal of Heat Transfer*, Vol. 112, No. 3, 1990, pp. 595–601.

[3]Beam, J. E., and Mahafekey, E. T., "Heat Transfer Visualization in the Double Wall Artery Heat Pipe," AIAA/ASME Thermophysics and Heat Transfer Conf., Boston, MA, June 2–4, 1986.

[4]Stalmach, D. D., Oren, J. A., and Cox, R. L., "Systems Evaluation of Thermal Bus Concepts," 2-53200/2r-53030, Vought Corp., Dallas, TX, Feb. 1984.

[5]Fleischman, G. L., "Osmotic Heat Pipe," Air Force Wright Aeronautical Lab., TR-81-31332, Wright-Patterson AFB, Dayton, OH, Nov. 1982.

[6]Narasaki, T., "The Characteristics of Bimorph Vibrator Pump," *Proceedings of the SAE Energy Conversion Engineering Conference*, San Franscisco, CA, Aug. 1978, pp. 2005–2010.

[7]Peterson, G. P., "Thermal Control Systems for Spacecraft Instrumentation," *Journal of Spacecraft and Rockets*, Vol. 24, No. 1, 1986, pp. 7–14.

[8]Chattock, A. P., Walker, W. E., and Dixon, E. H., *Philosophy Magazine*, Vol. 1, 1901, p. 79.

[9]Stuetzer, O. M., "Ion-Drag Pressure Generation," *Journal of Applied Physics*, Vol. 30, July 1959.

[10]Abu-Ramia, M. M., "Possible Applications of Electro-Osmotic Flow Pumping in Heat Pipes," 6th Thermophysics Conf., AIAA Paper 71-423, Tullahoma, TN, April 1971.

[11]Jones, T. B., "An Electrohydrodynamic Heat Pipe," ASME Winter Annual Meeting, New York, Nov. 1972, pp. 26–30.

[12]Kawahira, H., Kubo, Y., Yokoyama, T., and Ogata, J., "The Effect of an Electric Field on Boiling Heat Transfer of Refrigerant-11–Boiling on a Single Tube," *IEEE Transactions On Industry Applications*, Vol. 26, April 1990.

[13]Yabe, A., Mori, Y., and Hijikata, K., "Heat Transfer Enhancement Techniques Utilizing Electric Fields," *Heat Transfer in High Technology and Power Engineering*, Hemisphere, Washington, DC, 1987.

[14]Castaneda, J. A., and Seyed-Yagoobi, J., "Electrohydrodynamic Pumping of Refrigerant 11," *Proceedings of the IEEE-IAS Annual Meeting*, Dearborne, MI, Sept. 1991, pp. 500–503.

[15]Chi, S. W., *Heat Pipe Theory and Practice*, McGraw-Hill, New York, 1976.

[16]Dunn, P. D., and Reay, D. A., *Heat Pipes*, 3rd ed., Pergamon, New York, 1982.

[17]Crowley, J. M., *Fundamentals of Applied Electrostatics*, Wiley, New York, 1986, p. 156.

[18]Seyed-Yagoobi, J., Castaneda, J. A., and Bryan, J. E., "Theoretical Analysis of Ion-Drag Pumping," *Proceedings of the IEEE-IAS Annual Meeing*, Houston, TX, Oct. 1992, pp. 1412–1418.

[19]Babin, B. R., "Enhancement of Heat Pipes with Ion-Drag Pumps," M.S. Thesis, Mechanical Engineering Dept., Texas A&M Univ., College Station, TX, 1991.